Garg, D. R., and D. M. Ruthven, "Sorption of CO_2 in Davison 5A Molecular Sieve," *Chem. Eng. Sci.*, **30**, 436 (1975).
Gilmer, H. B., and Riki Kobayashi, "The Study of Multicomponent Gas Solid Equilibrium at High Pressures by Gas Chromatography: Part II. Generalization of the Theory and Application to the Methane-Propane-Silica Gel System," *AIChE J.*, **11**, 702 (1965).
Hattaway, R. D., "A Chromatographic Study of the Diffusion and Adsorption of Methane, Ethane, and Propane in a Synthetic Zeolite," Ph.D. thesis, Rice Univ., Houston, Tex., (Oct., 1973).
Haydel, J. J., "Development of Gas Chromatography to Study High Pressure Multicomponent Adsorption Equilibria: Application to the Methane-Propane-Silica Gel System," Ph.D. thesis, Rice Univ., (Dec., 1965).
Hori, Y., and Riki, Kobayashi, "Thermodynamic Properties of the Adsorbate for High Pressure Multilayer Adsorption," *Ind. Eng. Chem. Fundamentals*, *12*, No. 1, 26 (1973).
———, "High Pressure Adsorption: The Adsorption of Methane on Porasil at Low Temperatures and Elevated Pressures by Gas Chromatography," *J. Chem. Phys.*, **54**, No. 3, 1226 (1971).
Horn, F. J. M., "Calculation of Dispersion Coefficients by Means of Moments," *AIChE J.*, **17**, No. 3, 613 (1971).
Kline, S. J., and F. A. McClintock, "Describing Uncertainties in Single Sample Experiments," *Mech. Eng.*, 3 (Jan., 1953).
Kobayashi, R., P. S. Chappelear and H. A. Deans, Physiochemical Measurements by Gas Chromatography," *Ind. Eng. Chem.*, **59**, No. 10, 63 (1967).
Lederman, P. B., and B. Williams, "The Adsorption of Nitrogen-Methane on Molecular Sieves," *AICh J.*, **10**, 30 (1964).
Loughlin, K. F., K. A. Holborrow and D. M. Ruthven, "Multicomponent Sorption Equilibria of Light Hydrocarbons in 5A Zeolite," *AIChE Symposium Ser. No. 152*, **71**, 24 (1974).
Martin, A. J. P., and R. L. M. Synge, "A New Form of Chromatogram Employing Two Liquid Phases, *Biochemical Journal*, 35, 1358 (1941).
Masukawa, S., and R. Kobayashi, "The Hypothetical Perfect Gas Perturbation and the Determination of the Volume of the Adsorbed Phase in Gas Solid Chromatographic Columns," *J. Gas. Chrom.*, **6**, 257 (1968).
Riekert, L., "Sorption Diffusion and Catalytic Reaction in Zeolites," *Adv. Catalysis*, **21**, 281 (1970).
Ruthven, D. M., "Simple Theoretical Adsorption Isotherm for Zeolites," *Nature Phys. Sci.*, **232**, No. 29, 70 (1971).
———, "Sorption of Oxygen, Nitrogen, Carbon Monoxide, Methane, and Binary Mixtures of These Gases in 5A Molecular Sieve," *AIChE J.*, **22**, No. 4, 753 (1976).
———, K. F. Loughlin and K. A. Holborrow, "Multi-component Sorption Equilibrium in Molecular Sieve Zeolites," *Chem. Eng. Sci.*, **28**, No. 3, 701 (1973).
Starling, K. E., *Fluid Thermodynamic Properties for Light Petroleum Systems*, Gulf Publishing Company, Houston, Tex. (1973).

Manuscrpt received September 7, 1979; revision received January 2, and accepted January 23, 1980.

Throughflow Drying and Conditioning of Beds of Moist Porous Solids: A Simple Method for the Quantitative Prediction of Moisture and Temperature Fronts

A simple procedure previously developed for the prediction of fixed bed adiabatic sorption operations (Basmadjian, 1980*b*) has been extended to the throughflow drying and conditioning of beds of moist porous solids. The method eliminates time consuming numerical solutions of the model PDE's and yields satisfactory agreement with reported experimental data.

DIRAN BASMADJIAN

Department of Chemical Engineering and Applied Chemistry University of Toronto Toronto, Ontario M5S 1A4

SCOPE

The simulation of moisture and temperature fronts which arise in throughflow drying and ventilating of fixed beds of moist porous solids has previously required the numerical solution of coupled partial differential equations together with analytical expressions for the complex moisture isotherms. Even for persons experienced in numerical work, the task can easily occupy several days of fairly laborious work. These drawbacks are overcome here by means of a simple two-step procedure. The rigorous equilibrium mass and energy balances are combined with plots of moisture isotherms to carry out a graphical construction of the adiabatic, or effective equilibrium curves. Tabulated solutions for isothermal sorption are then applied along these curves to derive nonequilibrium moisture and temperature profiles or breakthrough curves. The procedure requires less than an hour's unskilled work once the relevant thermal, kinetic and equilibrium data are known.

In the absence of kinetic data, step 1 also provides an easy means of deriving equilibrium bed profiles, establishing the nature of the moisture fronts (stable or expanding) and estimating the length of the plateau zone. These procedures can be used for a rapid analysis of bed behavior over the entire domain of operations and are useful in estimating drying times as well as material and energy consumption.

0001-1541-80-3895-0625-$01.25.

CONCLUSIONS AND SIGNIFICANCE

It has been shown that a simple graphical construction of adiabatic vapor-solid equilibrium curves can be combined with existing solutions for fixed bed isothermal sorption to arrive at reasonably accurate predictions of the throughflow drying and conditioning of beds of moist porous particles. Calculated profiles and breakthrough curves agree with computer solutions of the relevant conservation and equilibrium relations and predict reported experimental data within the limits of accuracy of the physical parameters.

A good many drying operations in present day use involve passing an air stream through a fixed bed of particulate solids. This mode of operation, using heated, ambient or chilled air, finds extensive application in agriculture for the purpose of drying or ventilating grain crops prior to or during storage (Brooker et al., 1974). Other applications range from the regeneration of desiccants to a recent pilot plant for the large scale drying of municipal and agricultural wastes (Meiering et al., 1972).

In these operations, one is primarily interested in calculating moisture and temperature distributions, drying times and power consumption. The model equations describing the process consist of two coupled nonlinear PDE's derived from differential mass and energy balances and an appropriate analytical expression for the moisture isotherms. The major simplifications commonly used in these models postulate adiabatic operation, plug flow and negligible bed shrinkage, as well as uniform initial and inlet conditions. Heat and mass transfer resistances are incorporated to varying degrees, but these are nearly always expressed through simple linear driving force rate equations.

Even with these simplifications, it is generally necessary to resort to numerical solutions of the model equations. A first such solution which included both heat and mass transfer resistances was given by Van Arsdel (1955), who used the results to analyze the drying of food products. Subsequent simulations have been concerned chiefly with the drying of various grain crops (Boyce, 1965; Bakker-Arkema, 1967; Myklestad, 1968; Spencer, 1969, 1972; O'Callaghan et al., 1971; Brooker et al., 1974; Ingram, 1976) and moisture transfer in ventilated beds of textile fibers (Nordon, 1964, 1965). The same systems have also been analyzed using equilibrium models in which heat and mass transfer resistances are neglected (Nordon and Bainbridge, 1972; Banks, 1972; Sutherland et al., 1972). The results of this approach are less quantitative but afford a broader and more comprehensive analysis of nonisothermal fixed bed processes (Pan and Basmadjian, 1971; Basmadjian et al., 1975).

The chief drawback in these simulations, whether based on equilibrium or nonequilibrium models, is the length of the numerical computations involved. The fitting of analytical expressions to the complex equilibrium data can be particularly onerous, involving at times as many as six equations, even over a modest temperature range of 50°C (Brooker et al., 1974, p. 254). Clearly, these methods are not suited for a rapid analysis of drying processes or engineering estimates of important design parameters.

A similar lack of convenient methods for analyzing adiabatic sorption prompted us recently to devise a simple graphical-algebraic procedure which allows the rapid derivation of sorption profiles and breakthrough curves (Basmadjian, 1980*b*). In the first part of the two-step procedure, a simple graphical construction is used to obtain the adiabatic or effective, equilibrium curves in a $q - Y$ diagram (solid phase vs. gas phase concentration). These curves are based on the rigorous equilibrium conservation equations and make direct use of equilibrium data in their graphical form. They also permit the rapid construction of equilibrium bed profiles or breakthrough curves which would previously have required a numerical solution of the relevant model equations. In the second step of the procedure, nonequilibrium profiles and breakthrough curves are derived by applying well-established solutions for isothermal sorption along the adiabatic equilibrium curves. Interphase heat transfer resistance has to be neglected in this procedure, but the treatment is otherwise quite general and capable of accommodating various types and combinations of mass transfer resistance.

The agreement we obtained with adiabatic fixed bed sorption data encouraged us to extend the method to convective drying and other fixed bed moisture transfer operations. These processes, though similar to the sorption operations, have distinct applications as well as unique characteristics of their own which require a separate treatment.

CONSTRUCTION OF ADIABATIC EQUILIBRIUM CURVES, BED PROFILES AND BREAKTHROUGH CURVES

The equilibrium mass and energy balances for the fixed bed drying or remoistening of solids are represented by the following two coupled PDE's:

$$G_b \frac{\partial Y}{\partial z} + \rho_b \frac{\partial q}{\partial t} = 0 \tag{1}$$

$$G_b \frac{\partial}{\partial z}[\bar{C}_{pb}(T - T_r)] + \rho_b \frac{\partial}{\partial t}[\bar{C}_{ps}(T - T_r) + q\Delta H] = 0 \tag{2}$$

We had previously shown that these PDE's can be converted, via the method of characteristics, into two alternate forms which represent combined mass and energy balances [Pan and Basmadjian, 1971, Equations (17) and (23)]:

$$\frac{dq}{dY} = \frac{\bar{C}_{ps}}{\bar{C}_{pb}} + \frac{1}{\bar{C}_{pb}} \frac{d(q\Delta H)}{dT} \tag{3}$$

$$\frac{q - q_j}{Y - Y_j} = \frac{(\bar{C}_{ps})_j}{(\bar{C}_{pb})_j} + \frac{q\Delta H - (q\Delta H)_j}{(\bar{C}_{pb})_j (T - T_j)} \tag{4}$$

Both these combined conservation equations can be further recast into a common difference form, which is used as the basis for the graphical construction of the adiabatic equilibrium curves:

$$\frac{\Delta q}{\Delta Y} = \frac{a/b}{1/b - \Delta Y} \tag{5}$$

where $a = \bar{C}_{ps}/\bar{C}_{pb}$ and $b = \Delta H/\bar{C}_{pb}\Delta T$

An example of the construction scheme, along with the adiabatic equilibrium curves which result from it, are shown in Figures 1*a* and 1*b*. Further details will be found in our previous publication (Basmadjian, 1980*b*). The noteworthy feature here is that the construction almost invariably leads to two intersecting branches connecting inlet air and the initial state of the bed. In the example given (Figure 1), drying takes place, in the first instance, along the shallow branch of the curve, with an attendant decrease in temperature. After an intervening plateau of constant state represented by the point of intersection, the moisture decrease resumes along the steep branch of the equilibrium curve, accompanied by a rise in temperature to that of the inlet air. Bed profiles of this type, consisting of two fronts or zones moving at different velocities and separated by a plateau of constant temperature and concentration, occur with great frequency in moisture transfer operations. Not the least of the advantages of our graphical construction lies in its ability to convey these features at a glance.

The actual derivation of equilibrium temperature and concentration profiles from the preceding construction is a relatively simple matter. Some care must be exercised, however, in correctly identifying those portions of the adiabatic curve which lead to stable or shock moisture fronts (indicated by a step change in q, Y and T), and those which give rise to unstable or continuously broadening zones. A general guide to this problem is given in Figure 1 of our previous publication (Basmadjian, 1980*a*). It identifies the shallow branch of the adiabatic curve as a type I (Langmuir) equilibrium curve and the resulting profile as a broadening desorption front. By contrast, the steep branch of the adiabatic curve is identified as a type III equilibrium curve, and desorption along it leads to a stable shock discontinuity. The total equilibrium profile or breakthrough curve can then be constructed using the simple algebraic relations (Basmadjian, 1980*a*)

$$t/z = \frac{\rho_b}{G_b}(\Delta q_0/\Delta Y_0) \quad \text{for stable fronts} \qquad (6)$$

$$t/z = \frac{\rho_b}{G_b}(dq^*/dY) \quad \text{for broadening fronts} \qquad (7)$$

where $\Delta q_0/\Delta Y_0$ is the slope of the chord across a branch of the adiabatic equilibrium curve, and dq^*/dY the slope of the equilibrium curve itself. A construction of this kind is shown in Figure 1*c*.

We note that a large variety of different adiabatic equilibrium curves can arise in principle, including S shaped branches with inflection points similar to the well-known adsorption isotherms of types II, IV and V. The graphical guide previously cited provides extensive information on the construction of equilibrium sorption fronts in these more complex cases.

The exact form of the adiabatic curve is strongly dependent on the type and curvature of the moisture isotherms. Some simple predictions of its shape as a function of isotherm slopes can be made on the basis of equilibrium theory. These have been summarized in Appendix B and provide a means of assessing the type of moisture fronts to be expected for a particular type of isotherm.

CONSTRUCTION OF ADIABATIC NONEQUILIBRIUM BED PROFILES AND BREAKTHROUGH CURVES

Once the adiabatic equilibrium curves are established, solutions for isothermal nonequilibrium sorption can, in principle, be applied along these curves to describe adiabatic nonequilibrium bed behavior. In our previous publication dealing with adiabatic sorption (Basmadjian, 1980*b*), we chose for this purpose the Hiester-Vermeulen charts which are based on the Thomas kinetic treatment and have proven their validity in various isothermal contexts (Basmadjian, 1980*a*). In these charts, the operational parameters are expressed by means of the following dimensionless groups:

The mass balance or throughput parameter Z:

$$Z = \frac{\Delta Y_0 G_b \cdot t}{\Delta q_0 z \cdot \rho_b} \qquad (8)$$

The equilibrium separation factor r:

$$r = \frac{(\Delta Y/\Delta Y_0)(1 - \Delta q/\Delta q_0)}{(\Delta q/\Delta q_0)(1 - \Delta Y/\Delta Y_0)} \qquad (9)$$

which applies to adsorption along type I and desorption along type III equilibrium curves and has to be inverted for the reverse operations.

The number of reaction units N_R which incorporates the mass transfer resistance through the solid phase diffusivity D_s and particle radius R:

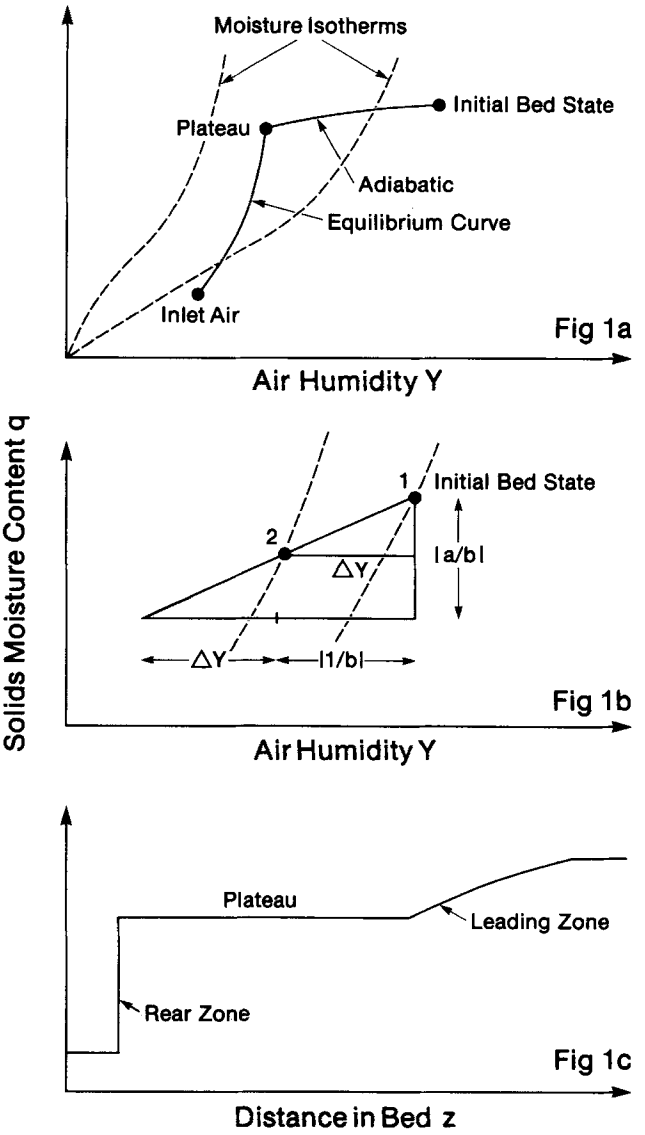

Figure 1. Construction of equilibrium bed profiles. *a*. A typical adiabatic equilibrium curve connecting initial bed and inlet air states. *b*. Initial step in the graphical construction of the adiabatic equilibrium curve [Equation (5)]. *c*. Equilibrium moisture profile based on Figure 1*a* and Equations (6) and (7).

$$N_R = 15\frac{D_s}{R^2}z\frac{\rho_b}{G_b}\frac{\Delta q_0}{\Delta Y_0}f(r) \qquad (10)$$

where $f(r) = 2/(1+r)$ for $0 < r < 1$
$= r^{-1/2}$ for $r \geq 1$

Δq_0 and ΔY_0 represent the difference in moisture content and air humidity over a particular branch of the adiabatic equilibrium curve. Charts are available for five dimensionless breakthrough ratios $\Delta Y/\Delta Y_0$ (Basmadjian, 1980*a*). Two of these for the critical ratios of 0.1 and 0.9 are reproduced for convenience in Figures 2 and 3.

Details of the application of these charts can be found in Basmadjian (1980*a*) and in the sample calculations which appear in Appendix A of this paper. We limit ourselves here to some additional comments of particular relevance to the operations under consideration.

Although the Hiester-Vermeulen charts present by far the most complete set of solutions for isothermal sorption, their application to drying operations revealed several deficiencies. They are, at present, limited to values of $N_R \geq 4$ and give direct readings only of the fluid breakthrough concentrations. To derive bed profiles, one generally has to apply a brief trial and error procedure, since the bed length z occurs in both N_R and Z (see in this connection the sample calculation in Appendix A). To overcome these drawbacks, we have prepared revised charts which will allow direct readings of both solid and fluid phase profile and breakthrough concentrations.* We note in this connection that in most drying studies, the diffusivity D_s contained in N_R is not measured directly but is reported in terms of a drying rate constant k extracted from an empirical thin layer rate equation:

$$\frac{\partial q}{\partial t} = k(q^* - q) \qquad (11)$$

This is the familiar logarithmic or linear driving force rate law, and it is common to relate k to the solid phase diffusivity via the well-known Glueckauf approximation (1955):

$$k = 15\frac{D_s}{R^2} \qquad (12)$$

k is generally a function of one or more of the state variables q, Y, T. To evaluate it for a particular moisture level, q and the corresponding Y are located on the operating line (Figure 4*b*), and the temperature is read from the adiabatic equilibrium curve at the same Y value. This procedure assumes a solid phase driving force and can be used for self-sharpening profiles only. For broadening fronts, no simple construction of the operating curve exists, and one must use the more detailed charts which allow a direct reading of both q and Y. In this work, such broadening fronts were encountered only on the shallow branch of the equilibrium curve which practically coincides with the operating curve. k evaluations can in this case be done directly on the equilibrium curve with little loss in accuracy.

A final comment concerns certain limitations imposed on the use of combined mass and energy balances as adiabatic equilibrium curves. It is seen from Equations (3) and (4) that their slope is limited by the heat capacity ratio C_{ps}/C_{pb}. We have found in our previous sorption study that this necessitates an additional construction when deriving self-sharpening moisture fronts from the steep branch of the adiabatic equilibrium curve. Both Equation (4) and the material balance given by the operating line (Figure 4*b*) must be used to establish the proper equilibrium temperature. This is done by choosing a pair of $q - Y$ values

Manuscript submitted to J. Agric. Eng. Res.

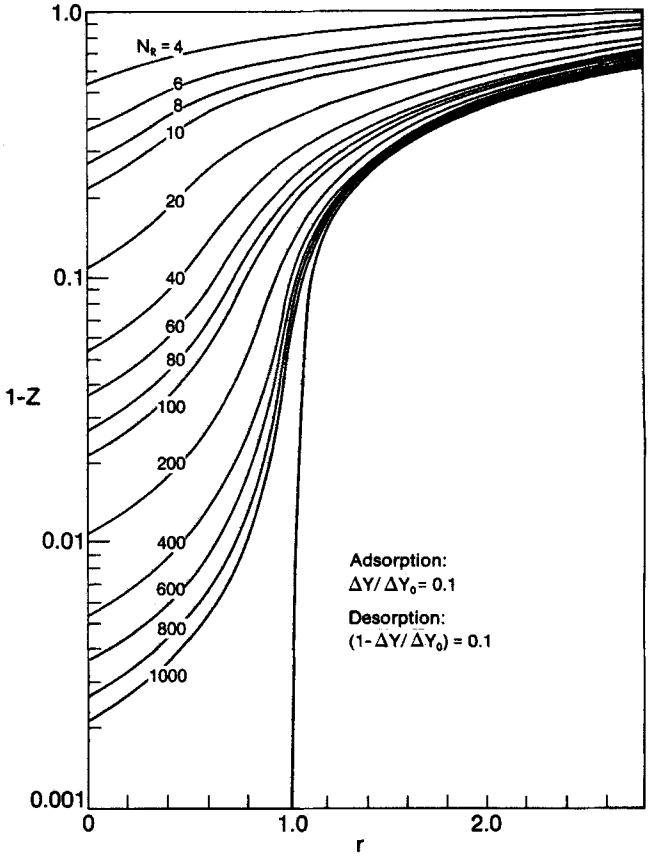

Figure 2. Plot of Hiester-Vermeulen parameters for a dimensionless humidity breakthrough ratio of 0.1, 0.9.

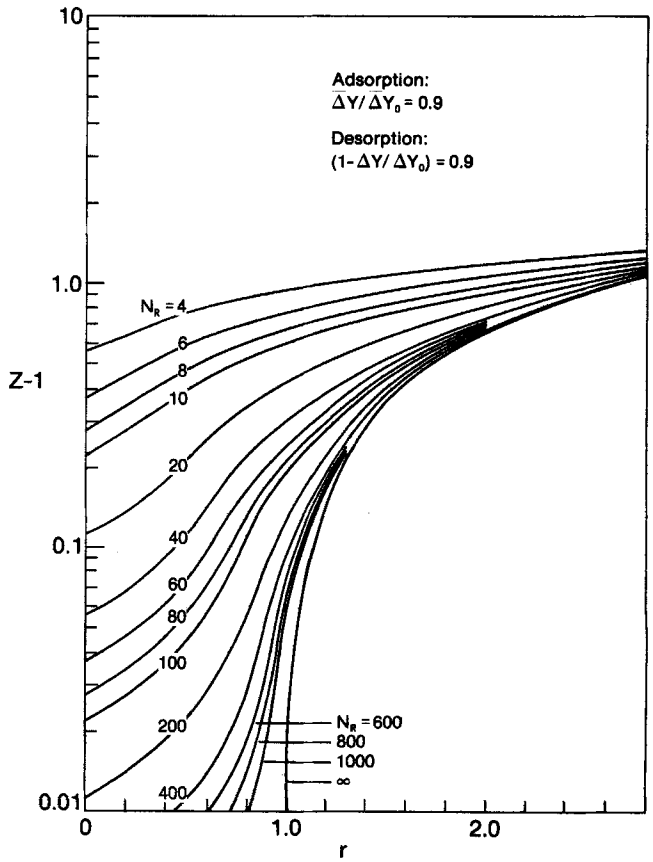

Figure 3. Plot of Hiester-Vermeulen parameters for a dimensionless humidity breakthrough ratio of 0.1, 0.9.

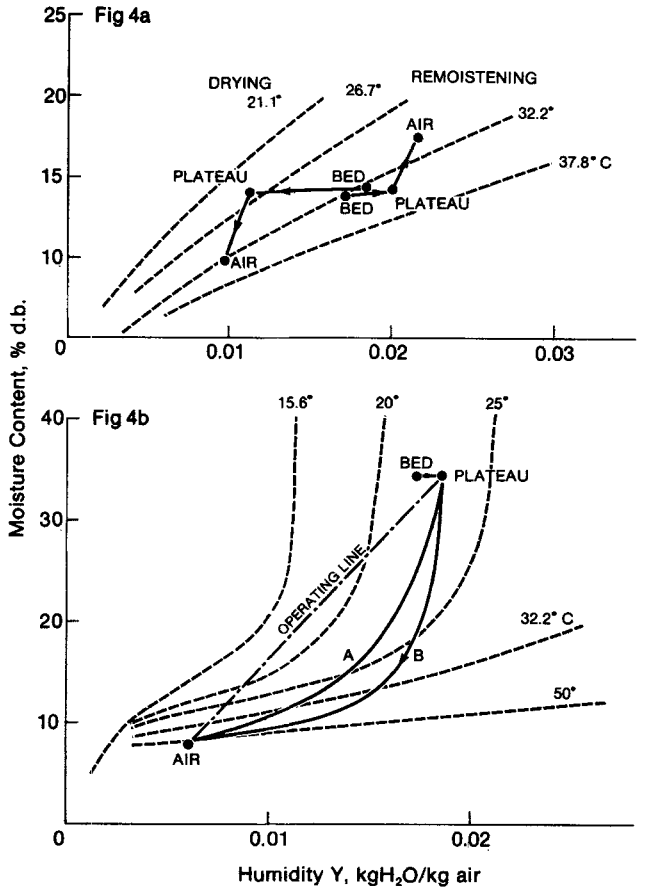

Figure 4. Selected operating diagrams. (———) adiabatic equilibrium curves. (-----) moisture isotherms. *a.* Conditioning of sorghum grain (Person et al., 1967). *b.* Drying of barley (Boyce, 1965). Curve A from Equation (5); curve B from Equation (13) and operating line.

on the operating line and substituting q into Equation (4), rearranged in the form

$$T = T_1 + \frac{(q\Delta H) - (q\Delta H)_1}{\frac{\Delta q_0}{\Delta Y_0}(\bar{C}_{pb})_1 - (\bar{C}_{ps})_1} \qquad (13)$$

where $\Delta q_0/\Delta Y_0$ is the slope of the operating line. The calculated temperature T and the humidity Y previously chosen locate a point on the appropriate branch of the adiabatic equilibrium curve. Three points between plateau and inlet air are usually sufficient to establish the complete curve (B in Figure 4*b*). Details are found in the sample calculation of Appendix A.

COMPARISON WITH EXPERIMENTAL RESULTS

Although the proposed method is of general validity, insufficient detail in many of the reported studies, as well as a lack of ancillary information, limited our choice of test data to a few well-documented grain and textile drying studies. These included the drying and chilling of wheat (Clark and Lamond, 1968; Sutherland et al., 1970, 1971), conditioning of sorghum (Person et al., 1967), drying of barley (Boyce, 1965), drying and conditioning of corn (Chittenden, 1961; Converse et al., 1973) and the drying and conditioning of wool (Nordon, 1965). Selected operating diagrams appear in Figure 4, and results of the first four studies are compared with our predictions in Figures 5 to 8. We have noted previously (Basmadjian, 1980*a*), as have Brooker et al. (1974, p. 203), that quantitative agreement with experimental results is well nigh impossible, and indeed to be viewed with some suspicion, because of

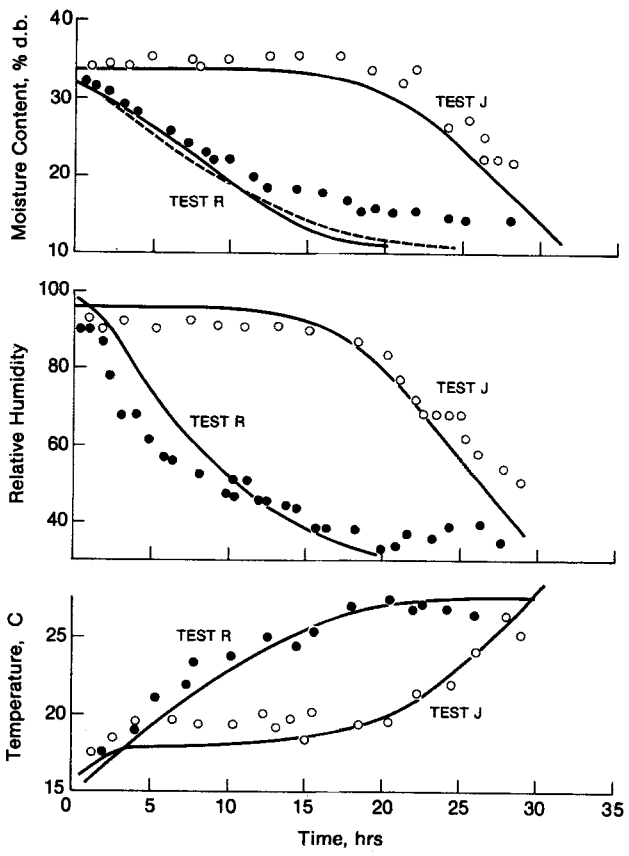

Figure 5. Comparison of experimental (⊙, ●) and predicted moisture, humidity and temperature at bed outlet. Data of Clark and Lamond (1965) for wheat. (———) predicted with k values from Eq'n (15). (-----) predicted with k values from Eq'n (14).

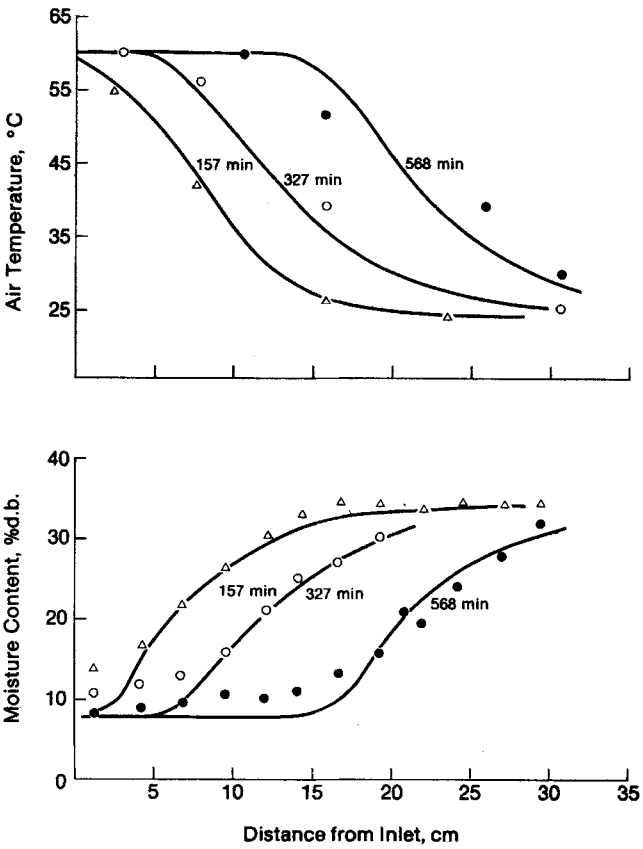

Figure 6 Drying of beds of barley, 0.305 m deep. (———) predicted profiles, (⊙, ●, △) data of Boyce (1965, run A) at various times.

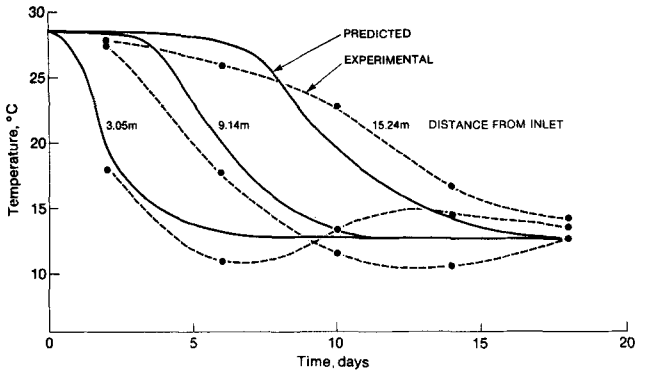

Figure 7. Temperature breakthrough curves in deep beds of chilled wheat. (———) predicted, ● data of Sutherland et al. (1970).

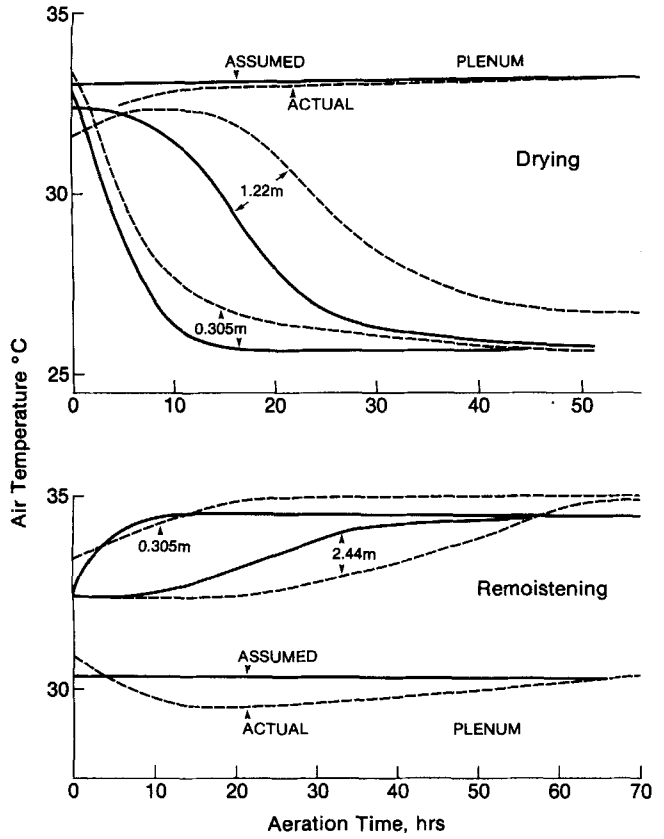

Figure 8. Exhaust temperatures during the conditioning of sorghum. (———) predicted, (-----) data of Person et al. (1967).

the inevitable errors in the ancillary data and bed measurements, as well as the assumptions inherent in these models. The results we report below should be viewed in this light.

The principal physical parameters for the construction of the equilibrium curves are summarized in Tables 1 and 2. Thermal parameters C_{ps} and ΔH come from the book of Brooker et al. (1974, pp. 85, 236). Equilibrium isotherms for wheat were constructed from data in the ASAE Handbook (Hahn, 1974) as well as from the equation proposed by Sutherland et al. (1971). The latter was used almost exclusively for our simulations of wheat and barley drying (Figures 5 to 7). For corn, we used the equilibrium data given by Brooker et al. (1974); for sorghum the data came from the ASAE Handbook (Hahn, 1974). The wool isotherms were derived from the analytical expression given by Nordon (1964).

No allowance was made for bed shrinkage or expansion. Dry bed densities ρ_b required in Equations (8) and (10) were calculated from

$$\rho_b = (\rho_b)_{wb}\,[1 - q_{wb}]$$

Values of $(\rho_b)_{wb}$ were generally available in the original studies.

In choosing rate laws, we limited ourselves to simple logarithmic forms [Equation (11)], although other forms can be accommodated by means to be described in a separate paper. k values for wheat were calculated according to expressions proposed by Becker (1959) and O'Callaghan (1971):

$$k_{\text{wheat}} = 48\,322\,\exp(-6\,160/T\,(°\text{K}))\,\text{s}^{-1} \qquad (14)$$

$$k_{\text{wheat}} = 2\,000\,\exp(-5\,094/T\,(°\text{K}))\,\text{s}^{-1} \qquad (15)$$

$$k_{\text{barley}} = 139.3\,\exp(-4\,430/T\,(°\text{K}))\,\text{s}^{-1} \qquad (16)$$

We used the latter two for our wheat and barley simulations and Equation (16) for the aeration runs with sorghum as well. Differences in the results for wheat obtained with Equations (15) and (16) are relatively minor (see Figure 5). Corn drying rate constants were taken from Pabis and Henderson (1961), and for wool the diffusivities cited by Nordon et al. (1960) were directly substituted into Equation (10).

TABLE 1: DETAILS AND PARAMETERS OF DRYING EXPERIMENTS

Work of:	Clark & Lamond test J	Clark & Lamond test R	Boyce (1965) run A	Chittenden (1961)	Nordon (1965)
Bed:	Wheat		Barley	Corn	Wool
Length, m	0.61		0.305	0.61	0.016
Diameter, m	1.67 × 1.67		0.31 × 0.31	0.10	—
Density (dry), kg/m³	529	545	662	610	176
Initial moisture, % d.b.	33.8	32.5	34.16	20.71	9.22, 35.8
Temperature, °C	16	14	21	26.7	20
Specific heat, kJ/kgK	1.295 + 4.19 q		1.45 + 4.19 q	1.38 + 4.19 q	1.21 + 3.56 q
Inlet air:					
Humidity, kg/kg	0.0076	0.00667	0.0058	0.0142	0, 0.0049
Temperature, °C	32.2	27.2	60	49	20
Mass velocity, kg/m²s	0.145	0.505	0.0862	0.163	0.175 (?)
Velocity, m/s	0.126	0.435	0.082	0.15	0.156 (?)

Table 2. Details and Parameters of Aeration Experiments

Work of:	Person et al (1967) Drying	Person et al (1967) Remoistening	Converse et al (1973)	Sutherland et al (1970)
Bed:	Sorghum		Corn	Wheat
Length, m	3.05		1.53	20.2
Diameter, m	1.83		1.83	6.18
Density (dry), kg/m³	630		525	692
Initial moisture, % d.b.	14.5	14.0	26.6	12.4
Temperature, °C	33	32.2	32.2	28.3
Specific heat, kJ/kgK	1.86		$1.38 + 4.19\,q$	$1.295 + 4.19\,q$
Inlet air:				
Humidity, kg/kg	0.0095	0.0217	0.0026	0.0048
Temperature, °C	33	30	1.7	10
Mass velocity, kg/m²s	0.00946		0.0173	0.00835
Velocity, m/s	0.00812		0.0135	0.0070

Measurements of Clark and Lamond (1965)

These authors have reported the results of some twelve drying tests on beds of wheat 0.61 m deep. Air temperatures and velocities in these experiments ranged from 27° to 66°C and from 12 to 44 cm/s. Beds with initial moisture contents of 30 to 50% d.b. were used (Table 1). The breakthrough curves obtained were comprised mainly of long rear zones and plateaus, with the leading zone barely discernible because of its quick passage through the bed.

Figure 5 shows a comparison of predicted and experimental temperatures, relative humidities and moisture contents of the bed outlet for two of the tests. The remainder of the runs were also successfully simulated. The degree of agreement is similar to that reported by O'Callaghan et al. (1971) using numerical solutions of the model equations. The largest deviations occur in the moisture content of run R in which ambient air of 27.2°C was used. It is not certain whether this is due to erroneous rate constants and equilibrium data or to the appearance of a heat transfer resistance in the final stages of the drying process. We note that the rate constants, Equations (15) and (16), were derived for temperatures above 25° to 30°C and that they do not contain a dependence on moisture content which would more accurately reflect residual moisture removal.

Data of Boyce (1965)

The data in this work are reported as bed temperature and moisture profiles and are again composed of a single drying zone and plateaus of various lengths (Figure 6). The leading zone had evidently passed through the bed at the time of measurements, and at any rate would have been difficult to discern because of the close proximity of initial state and plateau (see operating diagram, Figure 4*b*).

The trailing edge of the drying zone is shown in greater detail here than in the runs of Clark and Lamond and points to a small but systematic underestimation of residual moisture near the bed inlet. This may again be attributed to errors in the equilibrium and rate data or alternatively to the appearance of a significant heat transfer resistance in the final stages of the drying process. The results show, nevertheless, that the omission of that resistance can still lead to reasonably reliable predictions of the course of drying. Sample calculations for this system appear in Appendix A.

Aeration Runs of Sutherland et al (1970), Person et al. (1967) and Converse et al. (1973)

Aeration refers to the slow ventilation with ambient or chilled air of large storage bins of grain crops and other agricultural products. The moisture and heat transfer which occur in these operations have not been modeled previously except in a limited way by equilibrium theory (Sutherland et al., 1971). The process is particularly challenging to model because the low air velocities often lead to substantial channeling and may give rise to a significant fluid phase resistance as well as axial dispersion effects. Channeling cannot be accommodated by the conventional fixed bed models used here, but we were able to estimate fluid film and axial dispersion effects using correlations given in our sorption paper (Basmadjian, 1980*a*). In each instance they were found to be insignificant in comparison to the internal particle resistance.

A comparison of predicted and experimental temperature breakthrough curves at various bed positions is shown in Figure 7 for the deep bed experiments of Sutherland et al. (1970). We note that in these and other aeration experiments, the observed moisture and temperature fronts are associated with the leading zone of the bed profile traced out by the shallow branch of the adiabatic equilibrium curve (see operating diagram, Figure 4*a*). The plateau and rear drying zone which dominate conventional drying profiles (Figures 5 and 6) are delayed here because of the much lower air velocities used. The predictions are nevertheless in reasonable agreement with the data when we consider the occasional fluctuations of ± 30% in air flow and other cited error sources. We chose an average value of 500 CFM (8.35×10^{-3} kg/m²s) based on the air flow recordings given in the paper and a cited value of about 1 CFM (1.67×10^{-5} kg/m²s) per ton of wheat. The plateau temperature of 12.5°C we obtained in this fashion is in reasonable agreement with the value of 13.5°C calculated by Sutherland et al. (1971) using equilibrium theory.

Agreement of our simulations with the data of Person et al. (1967) is somewhat less satisfactory (Figure 8). The predicted temperature curves show a systematic shift to lower breakthrough times. Similar discrepancies were found in simulations of the aeration experiments of Converse et al. (1963) with corn (not shown). Two possible causes of these differences in addition to the factors previously cited are the evolution of transpiration heat (Sorenson, 1975) and unavoidable heat leaks to and from the bin wall. Although the latter was well insulated (Person et al., 1967), it nevertheless has a substantial heat capacity of its own which could make itself felt in the 1.83 m diameter beds used in these studies. The much better agreement obtained with data from the 6.40 m diameter bed of Sutherland et al. lends some support to this suggestion.

Drying of Wool (Nordon, 1965)

In contrast to the deep bed studies cited above, the wool experiments were carried out with shallow layers

only 1.6 cm thick. Inlet air and beds with various moisture contents were used (Table 1). In spite of the shallow bed depth, well-developed temperature fronts were obtained in each case, with a distinct plateau flanked by a fast leading zone and a much slower rear drying zone. Nordon (1965) was able to simulate the data semiquantitatively using a fairly rigorous PDE model which included both heat and mass transfer resistances. Although somewhat arbitrary transport coefficients were used, some discrepancies remained, particularly in the speed of approach to equilibrium which the model consistently overestimated. Our own simulations which do not include a heat transfer resistance, gave results very similar to the calculated curves of Nordon. The discrepancies with the data remained. Nordon (1965) has attributed these to possible axial dispersion and nonuniformity of fibers and bed. The heat capacity and/or conductivity of the wall may have been additional contributing factors. Finally, in spite of the great care with which the experiments were carried out, a small amount of air was later discovered to have bypassed the bed (Nordon, 1975). Corrections to the air velocity would shift the predicted values in the right direction.

ACKNOWLEDGMENT

The author is indebted to John G. Smith for his expert advice on crop drying and to Dr. K.D. Ha for carrying out calculations in the initial stages of this work.

NOTATION

a	$= \bar{C}_{ps}/\bar{C}_{pb}$
b	$= \Delta H/\bar{C}_{pb}\,\Delta T$
C_{pa}	= specific heat of adsorbed moisture, kJ/kgK
$\bar{C}_{pb}$	= specific heat of moist air, kJ/kgK
C_{ps}	= specific heat of dry solid, kJ/kgK
$\bar{C}_{ps}$	$= C_{ps} + q\,C_{pa}$, specific heat of moist solid, kJ/kgK
D_s	= solid phase diffusivity, m/s²
G_b	= (dry) air mass velocity, kg/m²
ΔH	= mean integral heat of adsorption, kJ/kg water
$\Delta H'; \Delta\tilde{H}$	= isosteric heat of adsorption, kJ/kg water; kJ/mole water
k	= drying rate constant, Equation (11)
N_R	= dimensionless number of reaction units, Equation (10)
q	= moisture content, kg water/kg dry solid
q^*	= equilibrium moisture content, kg water/kg dry solid
q^*_Y	$= (\partial q/\partial Y)_T$
q^*_T	$= (\partial q/\partial T)_Y$
Δq_0	= moisture content difference between end points of equilibrium curve, kg water/kg dry solid
r	= dimensionless separation factor, Equation (9)
R	= particle radius, m; gas constant, J/mole °K, Equation (A 12)
t	= time, s
T	= temperature, °K
T_r	= reference temperature, °K
Y	= air humidity, kg water/kg dry air
Y^*_T	$= (\partial Y/\partial T)_q$, Equation (B 13)
ΔY_0	= air humidity difference between end points of equilibrium curve, kg water/kg dry air
z	= distance from bed inlet, m
Z	= dimensionless throughput parameter, Equation (8)
$\lambda_\pm$	= defined by Equation (B3)
ρ_b	= (dry) bed density, kg/m³
ρ_g	= (dry) air density, kg/m³

Subscripts

1	= inlet air conditions
j	= inlet air or initial bed state
wb	= wet base

LITERATURE CITED

Bakker-Arkema, F. W., W. G. Bickert and R. J. Patterson, "Simultaneous Heat and Mass Transfer During the Cooling of a Deep Bed of Biological Products under Varying Inlet Air Conditions," *J. Agric. Eng. Res.*, **12**, 297 (1967).

Banks, P. J., "Coupled Equilibrium Heat and Single Adsorbate Transfer in Flow Through a Porous Medium. I. Characteristic Potentials and Specific Capacity Ratios," *Chem. Eng. Sci.*, **27**, 1143 (1972).

Basmadjian, D., K-D. Ha and C. Y. Pan, "Non-isothermal Desorption by Gas Purge of Single Solutes in Fixed-Bed Adsorbers. I. Equilibrium Theory," *Ind. Eng. Chem. Process Design Develop.*, **14**, 328 (1975).

———, "Rapid Procedures for the Prediction of Fixed-Bed Adsorber Behavior. I. Isothermal Sorption of Single Gases with Arbitrary Isotherms and Transport Modes," *ibid.*, **19**, 129 (1980).

———, "Rapid Procedures for the Prediction of Fixed-Bed Adsorber Behavior. II. Adiabatic Sorption of Single Gases with Arbitrary Isotherms and Transport Modes," *ibid.*, 137 (1980).

Becker, H. A., "A Study of Diffusion in Solids of Arbitrary Shape," *J. Appl. Polymer Sci.*, **1**, 212 (1959).

Boyce, D. S., "Moisture and Temperature Changes with Position and Time During Drying," *J. Agric. Eng. Res.*, **10**, 333 (1965).

Brooker, D. B., W. F. Bakker-Arkema and C. W. Hall, *Drying of Cereal Grains*, AVI Publ. Co., Westport, Conn. (1974).

Chittenden, D., "Drying of Single Kernels and Deep Beds of Shelled Corn," Ph. D. thesis, Univ. Wisc., Madison (1961).

Clark, R. G., and W. J. Lamond, "Drying Wheat in Two Foot Beds. Part III. Exhaust Air Humidity," *J. Agric. Eng. Res.*, **13**, 323 (1968).

Converse, H. H., D. B. Sauer and T. O. Hodges, "Aeration of High Moisture Corn," *Trans. Am. Soc. Agric. Engrs.*, **16**, 696 (1973).

Glueckauf, E., "Theory of Chromatography Part 10. Formulae for Diffusion into Spheres and Their Application to Chromatography," *Trans. Faraday Soc.*, **51**, 1540 (1955).

Hahn, R. H., Jr., ed., *Agricultural Engineers Yearbook*, 21 ed., Am. Soc. Agric. Engrs., St. Joseph, Mich. (1974).

Ingram, G. W., "Deep Bed Drier Simulation with Intra-particle Moisture Diffusion," *J. Agric. Eng. Res.*, **21**, 263 (1976).

Meiering, A. G., W. H. Clifford and F. W. Bakker-Arkema, "Drying of a Bed of Composted Waste," *Trans. Am. Soc. Agric. Engrs.*, **15**, 116 (1972).

Myklestad, O., "An Analysis of Transient Flow of Heat and Moisture During Drying of Granular Beds," *Int. J. Heat Mass Transfer*, **11**, 675 (1968).

Nordon, P., B. H. Mackay, J. G. Downes and G. B. McMahon, "Sorption Kinetics of Water Vapor in Wool Fibers: Evaluation of Diffusion Coefficients and Analysis of Integral Sorption," *Text. Res. J.*, **30**, 761 (1960).

———, "A Model for Mass Transfer in Beds of Wool Fibres," *Int. J. Heat Mass Transfer*, **7**, 639 (1964).

———, "The Exchange of Water Between a Bed of Wool Fibres and a Permeating Air Stream," *Proc. 3rd Int. Wool Textile Research Conference, Paris*, **3**, 23 (1965).

———, and N. W. Bainbridge, "Heat and Moisture Exchange in Wool Beds: Equilibrium Theory in the Hygroscopic Range," *J. Text. Inst.*, **63**, 429 (1972).

———, private communication (1975).

O'Callaghan, J. R., D. J. Menzies and P. H. Bailey, "Digital Simulation of Agricultural Drier Performance," *J. Agric. Eng. Res.*, **16**, 223 (1971).

Pabis, S., and S. M. Henderson, "Grain Drying Theory: II. A Critical Analysis of the Drying Curve for Shelled Maize," *J. Agric. Eng. Res.*, **6**, 272 (1961).

Pan, C. Y., and D. Basmadjian, "An Analysis of Adiabatic Sorption of Single Solutes in Fixed Beds: Equilibrium Theory," *Chem. Eng. Sci.*, **26**, 45 (1971).

Person, N. K., J. W. Sorenson, W. E. McCune and P. Hobgood, "The Use of Conditioned Air for Maintaining Quality of Stored Sorghum Grain," *Re. B-1066*, Texas A & M University, Texas Agricultural Experiment Station (1967).

Sorenson, J. W., Jr., private communication (1975).

Spencer, H. B., "A Mathematical Simulation of Grain Drying," *J. Agric. Eng. Res.*, **14**, 226 (1969).

———, " A Revised Model of the Wheat Drying Process," *ibid.*, **17**, 189 (1972).

Sutherland, J. W., D. Pescod, M. Airah and H. J. Griffiths, "Refrigeration of Bulk Stored Wheat," *Austr. Refrig., Air Cond. and Heating*, 30 (Aug., 1970).

Sutherland, J. W., P. J. Banks and H. J. Griffiths, "Equilibrium Heat and Moisture Transfer in Air Flow Through Grain," *J.*

Agric. Eng. Res., 16, 368 (1971).
Van Arsdel, W. B., "Simultaneous Heat and Mass Transfer in a Nonisothermal System," *Chem. Eng. Progr. Ser. No. 16*, **51**, 47 (1955).

APPENDIX A. Sample calculation: run A of Boyce (1965)

1. Construction of adiabatic equilibrium curves (Figure. 4b)

a. Steep branch through air inlet point—curve A (Figure 4*b*)
The construction uses Equation (5):

$$\frac{\Delta q}{\Delta Y} = \frac{a/b}{1/b - \Delta Y}$$

where $a = \bar{C}_{ps}/\bar{C}_{pb}$, $b = \Delta H/\bar{C}_{pb}\Delta T$.

At the air inlet point, $q = 0.077$, $Y = 0.0058$ (Figure 4*b*). Using Table 1 and the tabulations of Brooker et al. (1974), one obtains

$$\text{Solid specific heat } \bar{C}_{ps} = 1.45 + 4.19\,q = 1.77 \text{ kJ/kgK}$$

$$\text{Air specific heat } \bar{C}_{pb} = 1.02 \text{ kJ/kgK}$$

$$a = \bar{C}_{ps}/\bar{C}_{pb} = 1.77/1.02 = 1.74$$

$$b = \Delta H/\bar{C}_{pb}\Delta T = -2\,940/1.02\,\Delta T = -2\,880/\Delta T$$

The construction proceeds in accordance with diagram C of Figure 1 (Basmadjian, 1980*b*).

b. Shallow branch through initial bed state
Here, $q = 0.3416$, so that an analogous calculation will yield

$$\bar{C}_{ps} = 1.45 + 4.19 \times q = 2.89 \text{ kJ/kgK}$$

$$\bar{C}_{pb} = 1.02 \text{ kJ/kgK}$$

$$\Delta H = -2\,620 \text{ kJ/kg}$$

$$a = \bar{C}_{ps}/\bar{C}_{pb} = 2.89/1.02 = 2.83$$

$$b = \Delta H/\bar{C}_{pb}\Delta T = -2\,620/1.02\,\Delta T = -2\,570/\Delta T$$

These values can again be retained unchanged, and the construction is carried out according to diagram D, Figure 1 of Basmadjian (1980*b*).

c. Steep branch through air inlet point—curve B (Figure 4*b*)
To obtain this curve, we choose a point on the operating line, $q = 0.21$, $Y = 0.161$, and substitute into Equation (13):

$$T = T_2 + \frac{(q\Delta H) - (q\Delta H)_1}{\frac{\Delta q_0}{\Delta Y_0}(C_{pb})_1 - (C_{ps})_1}$$

where $\Delta q_0/\Delta Y_0$ = slope of operating line = 21.6 (Figure 4*b*). Thermal parameters come from previous calculations and Brooker et al. One obtains

$$T = 60 + \frac{-588 - (-227)}{21.6 \times 1.02 - 1.77} = 42.2°\text{C}$$

The coordinates $T = 42.2$, $Y = 0.161$ locate a point on curve B. Two additional points obtained in similar fashion are sufficient to establish the entire curve, used to derive the nonequilibrium profiles.

2. Calculation of the Hiester-Vermeulen parameters

Since the leading zone has already passed through the bed, only the rear zone and plateau need to be considered. As an illustration, we calculate the parameter values required to find the bed position z of the dimensionless moisture ratio $(1 - \Delta q/\Delta q_0) = (1 - \Delta Y/\Delta Y_0) = 0.5$ for a breakthrough time of 327 min (Figure 6).

a. Separation factor r
The appropriate expression is given by Equation (9):

$$r = \frac{\Delta Y/\Delta Y_0(1 - \Delta q/\Delta q_0)}{\Delta q/\Delta q_0(1 - \Delta Y/\Delta Y_0)}$$

where the subscripted quantities are obtained from the equilibrium curve endpoints, that is, the plateau and the inlet air state. Thus, from Figure 4*b*

$$\Delta q_0 = 0.342 - 0.076 = 0.266$$

$$\Delta Y_0 = 0.0181 - 0.0058 = 0.0123$$

The value of Y at the dimensionless moisture ratio of 0.5 is read from the equilibrium curve $Y = 0.0171$ and subtracted from the plateau value:

$$\Delta Y = 0.0181 - 0.0171 = 0.0010$$

Substitution into Equation (8) yields

$$r = \frac{(0.001/0.0123)\,0.5}{0.5\,(1 - 0.001/0.0123)} = 0.081$$

b. Throughput parameter Z
Since z occurs in both parameters Z and N_R, an initial guess has to be made and refined by trial and error. We assume $z = 0.122$ m. From Equation (8) and the values given in Table 1, we obtain

$$Z = \frac{\Delta Y_0 G_b t}{\Delta q_0 \cdot z \cdot \rho_b} = \frac{0.0123\,(0.0862 \times 60)\,327}{(0.266)\,(0.122)\,(662)} = 0.97$$

c. Number of reaction units N_R—check of assumed value of z
The drying rate constant $k = 15\,D_s/R^2$ is evaluated from O'Callaghan's expression at a temperature previously established (1c above) 42.2°C. Substituting into Equation (16), we get

$$k = 139.3 \exp(-4430/315.4) = 1.11 \times 10^{-4}\ \text{s}^{-1}$$

Hence, from Equation (10)

$$N_R = k \cdot z \cdot \frac{\rho_b}{G_b}\frac{\Delta q_0}{\Delta Y_0}\frac{2}{1 + r}$$

$$= 1.11 \times 10^{-4} \cdot 0.122 \cdot \frac{622}{0.0862} \cdot \frac{0.266}{0.0123} \cdot \frac{2}{1 + 0.081} = 4.18$$

For this value of N_R and a separation factor of 0.081, Figure 4 of Basmadjian (1980*a*) yields $Z = 1$, which is sufficiently close to the value 0.97 obtained under 2b). Further refinement leads to a value of $z = 0.118$ m.

APPENDIX B. Slopes of Adiabatic Equilibrium Curves as a Function of Isotherm Curvature

Some a priori knowledge of the shape of the adiabatic equilibrium curves may be gained by examining the characteristic ODE's which arise in the transformation of the equilibrium conservation equations (Pan and Basmadjian, 1971):

$$\left(\frac{dq}{dY}\right)_{\text{I}} = \frac{\bar{C}_{ps}}{\bar{C}_{pb}}\left(1 - \frac{\Delta H'}{\lambda_-}\right) \tag{B1}$$

$$\left(\frac{dq}{dY}\right)_{\text{II}} = \frac{\bar{C}_{ps}}{\bar{C}_{pb}}\left(1 - \frac{\Delta H'}{\lambda_+}\right) \tag{B2}$$

where

$$\lambda_\pm = -\frac{1}{2q^*_T}[\bar{C}_{ps} - \bar{C}_{pb}q^*_Y - \Delta H' q^*_T]$$

TABLE B1. SLOPES OF ADIABATIC EQUILIBRIUM CURVES FOR VARIOUS ISOTHERM SHAPES

Isotherms:	Horizontal ($q_Y^* = 0$)	Vertical ($q_Y^* = \infty$)	Favorable ($q_{YY}^* > 0$)	Unfavorable ($q_{YY}^* < 0$)
Adiabatic curves:				
Shallow branch	0	$\dfrac{\bar{C}_{ps}}{\bar{C}_{pb} - \Delta H' Y_T^*}$	Likely always concave to Y axis	Likely always concave to Y axis
Steep branch	$\bar{C}_{ps}/\bar{C}_{pb} + \Delta H' q_T^*/\bar{C}_{pb}$	∞	Concave or convex to Y axis	Always convex to Y axis

Note: $Y_T^* = -\dfrac{Y(29Y + 18)\,\Delta H'}{RT^2}$ for air-water-solid system

$$+\frac{1}{2q^*_T}[(\bar{C}_{ps} - \bar{C}_{pb}q^*_Y - \Delta H' q^*_T)^2 + 4\bar{C}_{ps}\Delta H' q^*_T]^{1/2} \qquad \text{(B3)}$$

and $\Delta H'$ = isosteric heat of adsorption. The equilibrium relation is formally represented by

$$q = q^*(Y, T) \qquad \text{(B4)}$$

and derivatives of this function are described by the subscripted symbols q^*_T and q^*_Y.

$$\left(\frac{dq}{dY}\right)_{\text{I}} \quad \text{and} \quad \left(\frac{dq}{dY}\right)_{\text{II}}$$

are the slopes of the shallow and steep branches of the equilibrium curve. Strictly speaking, these curves are applicable to broadening profiles only, but as mentioned in the previous sorption paper, they do not differ signficantly from the equilibrium curves generated by the algebraic shock equations. The results of our analysis can therefore be considered as having general validity. Equations (B1) to (B3) are used below to derive slopes of the adiabatic equilibrium curves for horizontal and vertical isotherms, as well as for the general case of an unfavorable isotherm.

Horizontal isotherms ($q_Y^* = 0$)

Expressions for this limiting case are derived by direct substitution of $q_Y^* = 0$ into the characteristic roots $\lambda_\pm$ [Equation (B3)] and are in turn used in Equations (B1) and (B2) to evaluate the slopes of the equilibrium path. One obtains for the shallow branch:

$$\lambda_- = \Delta H'; \left(\frac{dq}{dY}\right)_{\text{I}} = 0 \qquad \text{(B5)}$$

for the steep branch:

$$\lambda_+ = -\bar{C}_{ps}/q_T^* \; ; \left(\frac{dq}{dY}\right)_{\text{II}} = \frac{\bar{C}_{ps}}{\bar{C}_{pb}}\left(1 + \frac{\Delta H' q_T^*}{\bar{C}_{ps}}\right) \qquad \text{(B6)}$$

Vertical isotherms ($q_Y^* = \infty$)

Here is it convenient to express the characteristic roots $\lambda_\pm$ in an alternate form obtained by factoring out q_Y^* and eliminating q_T^* via the relation

$$q_Y^*/q_T^* = -1/Y_T^* \qquad \text{(B7)}$$

where Y_T^* is finite and is defined by the equilibrium relation

$$Y = Y^*(q, T) \qquad \text{(B8)}$$

The result is given by

$$\lambda_\pm = \frac{1}{2}\{\bar{C}_{ps}/Y_T^* q_Y^* - \bar{C}_{pb}/Y_T^* + \Delta H'$$

$$\pm[(\bar{C}_{ps}/Y_T^* q_Y^* - \bar{C}_{pb}/Y_T^* + \Delta H')^2 - 4\bar{C}_{ps}\Delta H'/Y_T^* q_Y^*]^{1/2}\} \qquad \text{(B9)}$$

Substituting $q_Y^* = \infty$ into (B9) and recalling the general requirement $(dq/dY)_{\text{II}} \geq \bar{C}_{ps}/\bar{C}_{pb} \geq (dq/dY)_{\text{I}}$ (Pan and Basmadjian, 1971), we obtain

for the shallow branch:

$$\lambda_- = \Delta H' - \bar{C}_{pb}/Y_T^*; \left(\frac{dg}{dY}\right)_{\text{I}} = \bar{C}_{ps}/(\bar{C}_{pb} - \Delta H' Y_T^*) \qquad \text{(B10)}$$

for the steep branch:

$$\lambda_+ = 0; \quad \left(\frac{dq}{dY}\right)_{\text{II}} = +\infty \qquad \text{(B11)}$$

We note that Y_T^* in Equation (B10) may be eliminated via the Clapeyron relation applicable to sorption systems

$$RT^2 = \left(\frac{d\ln p}{dT}\right)_q = -\Delta \bar{H}' \qquad \text{(B12)}$$

which, upon conversion of $\Delta \bar{H}'$ and the partial pressure of water vapour p to mass units yields

$$\left(\frac{\partial Y}{\partial T}\right)_q = Y_T^* = -\frac{Y(29Y + 18)\,\Delta H'}{RT^2} \qquad \text{(B13)}$$

Unfavorable isotherms ($q_{YY}^* > 0$)

No general prediction can be made for the curvature of the shallow branch in this case, although extensive calculations indicate the curve to be invariably concave to the Y axis. For the steep branch, a more rigorous statement is possible. We first note that T decreases with increasing q along this curve and that consequently q_Y^* will always increase in that direction, given an unfavorable isotherm. The derivative Y_T^* behaves identically, as can be seen from the expression (B13). Both q_Y^* and Y_T^* may thus be regarded as increasing with an increase in q or Y. It is then a matter of simple inspection of Equation (B9) for λ_+, and Equation (B2), to prove that the slope of the steep branch will increase in this direction, provided $\bar{C}_{ps}$ and $\bar{C}_{pb}$ are assumed constant.

Favorable isotherms ($q_{YY}^* < 0$)

No predictions are possible in this domain. Our previous work (Pan and Basmadjian, 1971; Basmadjian et al, 1975*a*) shows that the steep branch can be of arbitrary shape, while the shallow branch appears to be invariably concave to the Y axis.

A summary of the results of this analysis appears in Table B1.

Manuscript received July 6, 1979; revision received February 21, and accepted February 22, 1980.